Thermochimica Acta, 155 (1989) 163–186
Elsevier Science Publishers B.V., Amsterdam – Printed in The Netherlands

LOCALIZATION AND CHARACTERIZATION OF INTRACELLULAR LIQUID–LIQUID PHASE SEPARATIONS IN DEEPLY FROZEN *POPULUS* USING ELECTRON MICROSCOPY, DYNAMIC MECHANICAL ANALYSIS AND DIFFERENTIAL SCANNING CALORIMETRY

ALLEN HIRSH

American Red Cross, Holland Laboratories, 15601 Crabbs Branch Way, Rockville, MD 20855 (U.S.A.)

THOMAS BENT

Materials Testing Laboratory, Comsat Corporation, Clarksburg, MD 20874 (U.S.A.)

ERIC ERBE

Electron Microscope Laboratories, USDA BARC, Beltsville, MD 20705 (U.S.A.)

(Received 28 March 1989)

ABSTRACT

Populus balsamifera var. *virginiana* (Sargent), balsam poplar, is capable of withstanding liquid nitrogen temperatures when cooling is slow (less than $6\,^{\circ}C\ h^{-1}$) and the twigs are winter dormant. Cooling to $-50\,^{\circ}C$ at rates as high as $42\,^{\circ}C\ h^{-1}$ is also tolerated.

The mechanical behavior during warming of dormant twigs cooled at rates varying from $3\,^{\circ}C\ h^{-1}$ to $600\,^{\circ}C\ h^{-1}$ has been investigated using resonance mode dynamic mechanical analysis (DMA). The results were correlated with those of freeze-etch electron microscopy investigations of the samples as well as differential scanning calorimetry (DSC) of model solutions.

The results of these investigations were compared with mortality data on the twigs. This has led us to hypothesize that at critical cooling rates below $0\,^{\circ}C$ plasma membranes tear, leading to the rapid growth of intracellular ice. This in turn prevents the intracellular liquid–liquid phase separations seen by DMA in samples cooled at sublethal rates. DSC analysis of salt–sugar–protein model solutions supports the idea that when liquid–liquid phase separation does occur, some domains are sugar-depleted but rich in protein, while others are sugar-rich but low in protein. This may have important implications regarding the organization of extreme freezing resistance mechanisms in this natural system.

INTRODUCTION

Populus balsamifera var. *virginiana* (Sargent), balsam poplar, is one of a small group of woody plants native to the northern hemisphere which can withstand liquid nitrogen temperatures while in the winter dormant state.

0040-6031/89/$03.50

Our previous studies combining differential scanning calorimetric (DSC) analysis and freeze-fracture freeze-etch electron microscopy (EM) of frozen wood samples have shown that the intracellular fluids of the *Populus* form aqueous glasses free of ice crystals when the temperature falls below $-30\,^{\circ}C$ at cooling rates of $\leqslant 0.5\,^{\circ}C\ min^{-1}$. These initial studies showed that the primary glass-forming behavior appeared to closely mimic that observed by DSC in frozen solutions of raffinose and stachyose, storage sugars which are present in very high concentration in the intracellular fluids of the dormant wood [1–4].

The present work reports on further studies of frozen wood utilizing DSC, EM and dynamic mechanical analysis (DMA). The use of mechanical analysis has allowed us to confirm earlier DSC observations. In addition, it has provided us with evidence that liquid–liquid phase separations occur in the cytoplasm during slow cooling, leading to domains that are protein-rich but sugar-depleted and vice versa. We present evidence that phase separation of these domains can be inhibited and the intracellular solutions destabilized to allow ice formation during warming (devitrification) by cooling at lethal rates from the unfrozen state.

EXPERIMENTAL

Dynamic mechanical analysis

DMA measures the elastic properties of a sample: specifically, the moduli of energy stored (E') and lost (E'') in a sample as a function of temperature, amplitude of induced bending and induced frequency of bending. In the Dupont 982 system (Dupont, Wilmington, Delaware) bending frequency is at the resonant frequency of the sample and thus appears as a dependent variable. Our measurements were made in the frequency range 10–45 Hz. Mechanical transitions are most easily identified by calculation of $\tan\delta$, the ratio of the loss modulus to the storage modulus. Peaks in this curve indicate sudden changes in sample viscosity, and can be used to identify phase transitions.

Wood samples were prepared for DMA or EM analysis by placing 5 or 6 twigs of approximate dimensions 4–6 mm (diameter) × 25–50 mm (length) in a sealed centrifuge tube with several small pieces of ice in contact with the twigs. These tubes were then placed in an LT-50 or ULT-80 cooling bath (Neslab, Portsmouth, N.H.) and cooled at the rate appropriate for the experiment. When the bath had reached the appropriate temperature for each experiment the twigs were removed to liquid nitrogen and stored or transported to Comsat Corporation Laboratories. Prefrozen twigs were loaded in the mechanical stage of the DMA and kept at LN_2 temperatures by pouring LN_2 over them during the few seconds it took to load the twigs into the DMA. A precooled dewar shroud was then mounted around the

assembly to maintain temperatures below $-140\,^{\circ}C$, and the twigs allowed to equilibrate below $-150\,^{\circ}C$ for 20 min. Heating and the collection of data commenced simultaneously. Heating was monitored, but passive in early experiments until the temperature exceeded $0\,^{\circ}C$. The rate of heating thus obtained was not linear but much slower than with the heater on. The slow rate improved both the sensitivity of measurement and the accuracy of temperature measurement. Both temperature and time bases were recorded. In the temperature range -100 to $-50\,^{\circ}C$ the DMA heating rate averaged 1.0–0.5 °C min^{-1}. In the range -50 to $0\,^{\circ}C$ the rate was 0.5–0.2 °C min^{-1}. The samples for DMA were almost always ~ 25 mm (length) × ~ 5 mm (diameter). In several later experiments a new LN_2-based cooling system (LNCA, Dupont) allowed us to warm slowly and linearly over part of the temperature range.

Differential scanning calorimetry

Samples were placed in sealable aluminum pans (Perkin–Elmer Cat. No. B0143021, B0143004, Norwalk, Conn.), sealed immediately and weighed on an electronic balance (Perkin–Elmer Model No. AD-6). The samples were then placed in one cup of the head of a DSC–4 (Perkin–Elmer), with a sealed aluminum pan with or without ice in the other. Further details of the DSC operation may be found in a previous publication [4].

Electron microscope samples

Twig samples for the electron microscope were frozen exactly as for the DMA studies. Twigs frozen at 3 or 42 °C h^{-1} to $-50\,^{\circ}C$ were cracked into small fragments in a metal cup sitting in dry ice. Fragments were transferred in tacky 57% glycerol at $-80\,^{\circ}C$, immediately covered with liquid nitrogen, and fractured therein with a sharp scalpel. Twigs frozen at 120 or 600 °C h^{-1} to $-150\,^{\circ}C$ were held continuously in LN_2. A special copper block was devised to clamp twigs under LN_2 and allow for fracturing under LN_2. In a modified Denton freeze-etch unit the prefractured twigs were transferred into a shrouded chamber precooled to $-110\,^{\circ}C$. They were equilibrated for 10 min at $-110\,^{\circ}C$, and then etched for 10 min at 10^{-6} Torr at $-90\,^{\circ}C$. Platinum shadowing and carbon backing were done at $-110\,^{\circ}C$. After the vacuum was broken 2% lexan in dichloroethylene was added to preserve replica integrity during acid dissolution of the tissue. Samples were examined in an H500H (Hitachi) transmission electron microscope at 80 keV. Further details have been described in a previous paper [3].

Survival tests

Survival was monitored by placing twigs on moist perlite in an enclosed container on a well lit shelf. For three weeks callus formation, bud break

and the health of all tissues (in terms of browning) was monitored. A twig was judged to have either: (a) survived showing no activity, as evidenced by no browning of cortical tissues, xylem or pith; (b) survived with callus formation and/or bud break; or (c) died. Survival as reported here is (a) plus (b).

RESULTS

Dynamic mechanical analysis

Figures 1(a)–(d) show the DMA warming records of freshly collected fully hardy samples of *Populus* cooled at 3, 42, 120 and 90 °C h^{-1} respectively. The first two rates are non-injurious, but 90 and 120 °C h^{-1} are completely lethal rates.

The material cooled at 3 °C h^{-1} (Fig. 1(a), shows $\tan\delta$ peaks at about −100, −37 and −22 °C. The storage modulus value at very low temperature $E'(-160)$ is 8 GPa, typical of hardy material cooled at non-lethal rates. The ratios of the storage moduli are $E'(-60)/E'(-160) = 0.69$ and $E'(-30)/E'(-60) = 0.67$. These low values imply significant liquefaction of intracellular content during warming to −30 °C. It should also be noted that the storage modulus is monotonic decreasing throughout the range.

The ratio

$$\frac{E''(\text{upper } \tan\delta \text{ maximum}) - E''(-160)}{E''(\text{lower } \tan\delta \text{ maximum}) - E''(-160)}$$

is also a measure of relative liquefaction. This ratio, which we abbreviate to $E''(u)/E''(l)$, is 1.4 in the 3 °C h^{-1} cooled wood. This indicates that both lower and upper $\tan\delta$ peak regions contribute substantially to increased liquidity during warming.The general loss modulus level E'' is low, with a low temperature peak maximum of 115 MPa and a high temperature maximum of 170 MPa.

The material cooled at 42 °C h^{-1} (Fig. 1(b)) is similar in several important aspects to the material cooled very slowly. The value of $E'(-160)$ is 9.8 GPa. However, the $\tan\delta$ peaks are at −100, −28, −17 and −5 °C. The ratios $E'(-60)/E'(-160)$ and $E'(-30)/E'(-60)$ are 0.69 and 0.66, respectively—very close to those for the 3 °C h^{-1} cooled material. The ratio $E''(u)/E''(l)$ is 2.36, which is significantly higher than for the 3 °C h^{-1} cooled wood. Also, the general level of E'' is higher, with a low temperature peak maximum at 135 MPa and a high temperature maximum at 270 MPa. Again, the storage modulus is monotonic decreasing throughout the range.

Figure 1(c) shows a sample cooled at the lethal rate of 120 °C h^{-1} to −160 °C. This was followed by 18 °C h^{-1} warming to −115 °C, and then passive warming. The value of $E'(-140)$ is 3.6 GPa, which is much lower

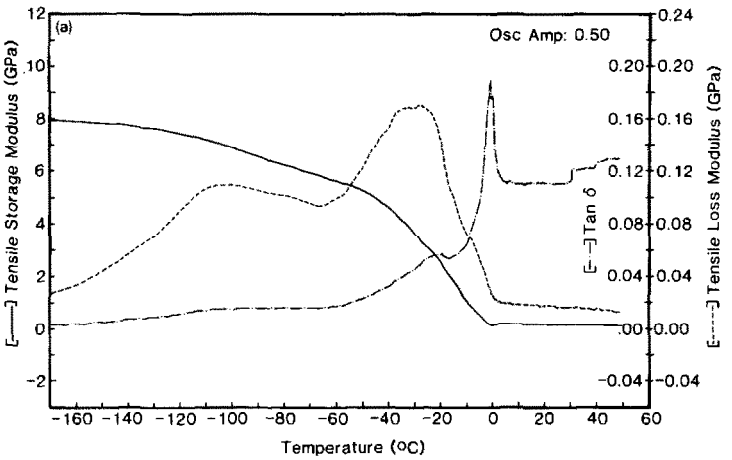

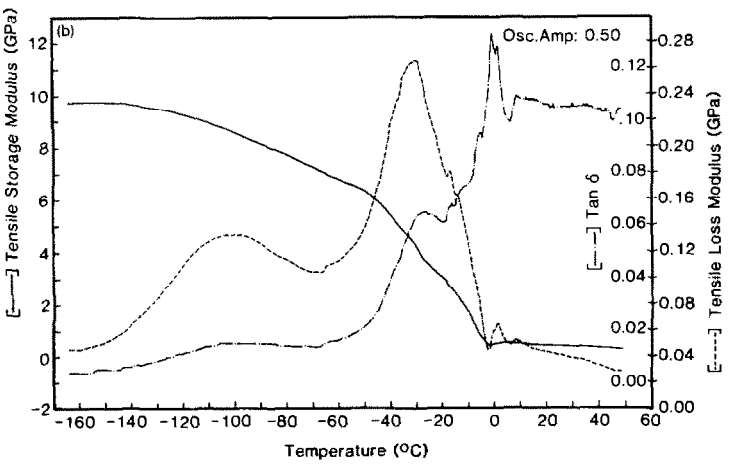

Fig. 1(a). Warming record after insertion in DMA at $-150\,^{\circ}$C of a fully cold hardy *Populus* twig, 25×5.35 mm. The twig was prefrozen to $-50\,^{\circ}$C at a mean rate of $3\,^{\circ}$C h^{-1}, then stored at $-80\,^{\circ}$C. The low temperature storage modulus is high at 8 GPa. E' has fallen to 5.5 GPa by $-60\,^{\circ}$C, and 3.5 GPa by $-30\,^{\circ}$C. E' is monotonic decreasing throughout the range, and falls to about 200 MPa above $0\,^{\circ}$C. The loss curve is complex, with peaks or shoulders at -107, -75, -45, -35, -28 and $-8\,^{\circ}$C. The comparatively simple $\tan\delta$ curve shows subzero peaks or shoulders at -100, -37 and $-22\,^{\circ}$C. Oscillation amplitude was 0.5 mm.

Fig. 1(b). A fully cold resistant 25×4.8 mm *Populus* twig was cooled in contact with ice to $-50\,^{\circ}$C at $42\,^{\circ}$C h^{-1}. It was then stored in dry ice. $E'(-160)$ is a very high 9.8 GPa; $E'(-60)$ is 6.7 GPa; $E'(-30)$ is 4.3 GPa. The final storage modulus above $0\,^{\circ}$C is about 300 MPa. Loss modulus data is complex, with subzero peaks or shoulders at about -100, -65, -35, -28, -17 and $-5\,^{\circ}$C. A considerable level of this complexity is also reflected in the $\tan\delta$ curve, with subzero peaks or shoulders at -100, -28, -17 and $-5\,^{\circ}$C. Despite the increased complexity, the basic structure of the curves is nearly identical to that for the $3\,^{\circ}$C h^{-1} cooled material. The storage modulus is monotonic decreasing throughout the range below $0\,^{\circ}$C. Oscillation amplitude was 0.5 mm.

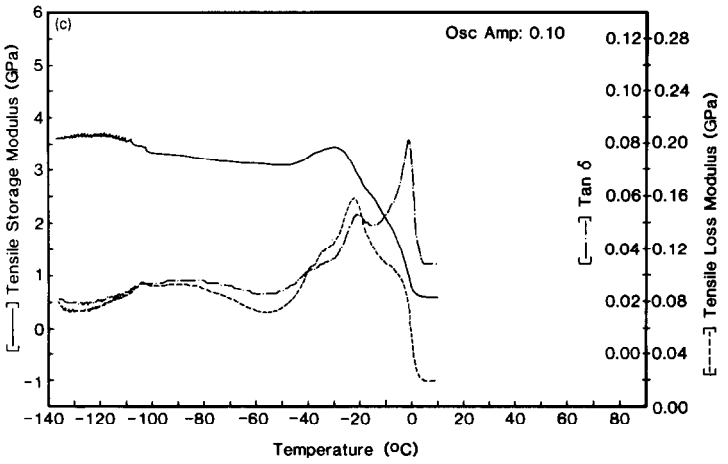

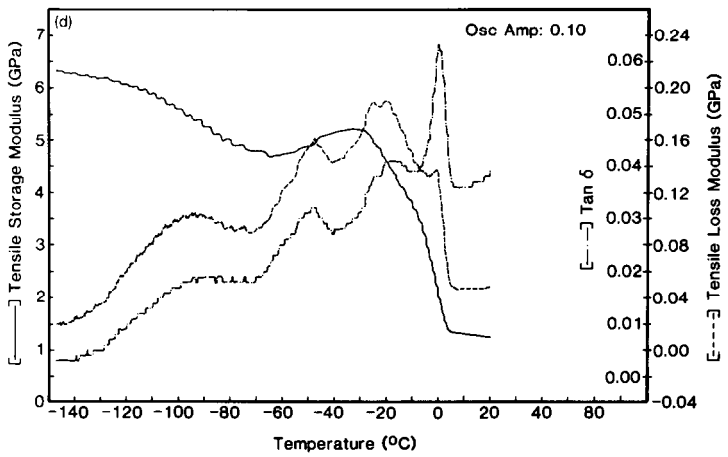

Fig. 1(c). A freshly collected fully hardy twig, 25×5.9 mm, was cooled to −150 °C in the DMA at 120 °C h^{-1}. The twig was warmed with working at 18 °C h^{-1} to −115 °C, and then free warming was begun. EM investigation of freshly collected twigs cooled at 20 °C h^{-1} indicates that this sample froze intracellularly during cooling. Note a low $E'(-140)$ of 3.6 GPa. Also note the slight increase in E' from −140 to −120 °C. Since this is near the T_g of pure water, this is likely to be crack healing in the intracellular glasses. E' remains almost level until −60 °C, then a gradual increase begins. The increase sharpens into a well defined devitrification peak between −50 and −30 °C. $E'(-30)$ is 3.35 GPa. E' above 0 °C is about 550 MPa. The corresponding loss curve shows subzero shoulders or peaks at −105, −90, −70, −40, −35, −21 and −5 °C. The very low temperature loss peak is greatly depressed. The tan δ curve shows peaks or shoulders at −105, −94, −40, −35 and −21 °C. The oscillation amplitude was 0.1 mm.

Fig. 1(d). Freshly collected fully hardy *Populus* twig, 25×5.5 mm, cooled to −150 °C at 1.5 °C min^{-1} with working. Warming commenced at 18 °C h^{-1} under LNCA control. Passive warming began at −70 °C. Regular oscillations during controlled warming are instabilities in the LNCA-982 electronic interface. The tan δ peaks at −95, −50, −25 and −20 °C are mirrored by corresponding loss peaks. The initial E' value is moderate at 6.4 GPa but increases in E' at higher temperatures indicate significant devitrification still occurred between −60 and −30 °C. Oscillation amplitude was 0.1 mm.

than for the slowly cooled samples. E' begins to increase immediately at $-140\,^{\circ}C$, and this stiffening persists until about $-120\,^{\circ}C$. The ratios $E'(-60)/E'(-140)$ and $E'(-30)/E'(-60)$ are 0.88 and 1.11, respectively —far higher than in samples cooled at a non-lethal rate. There are $\tan\delta$ peaks at -115 and $-94\,^{\circ}C$, a complex set of peaks between -40 and $-30\,^{\circ}C$, and a peak at $-21\,^{\circ}C$. The ratio $E''(u)/E''(l)$ is 5, which is also much higher than that for the slowly cooled samples. The low temperature E'' is very low, with a peak value of 95 MPa, whereas the high temperature E'' is 160 MPa. There is prominent stiffening of the sample above $-50\,^{\circ}C$, implying a significant devitrification in the temperature range -50 to $-30\,^{\circ}C$.

Figure 1(d) shows a sample cooled at $90\,^{\circ}C\ h^{-1}$ to $-150\,^{\circ}C$. This twig was worked (oscillating at resonance) while cooling. The DMA record shown here was obtained during controlled $18\,^{\circ}C\ h^{-1}$ warming from $-150\,^{\circ}C$ to $-70\,^{\circ}C$, followed by passive warming. The low temperature storage modulus $E'(-140)$ is 6.3 GPa, which is remarkably high for a twig cooled at lethal rates. However, this twig was worked while cooling and this may have allowed for considerable additional ice growth in the intracellular milieu. The cooling record (not shown) also showed considerable stiffening and cracking (sudden drops in E'). The ratio $E'(-60)/E'(-160)$ is 0.73, while $E'(-30)/E'(-60)$ is 1.12, which is good evidence of devitrification only at higher temperatures.

There are three clearly defined $\tan\delta$ peaks below the ice melting peak at $0\,^{\circ}C$. These are at -100, -48 and $-20\,^{\circ}C$. The ratio $E''(u)/E''(l)$ is a relatively low 2.1. However, the low temperature E'' peak is low at 105 MPa, while the high temperature maximum is 195 MPa.

Figures 2(a)–(c) show DMA records for wood from the same collection of twigs as shown in Figs. 1(c and d), but these twigs were stored for 7 months at $-20\,^{\circ}C$, then held for 16 days at $-5\,^{\circ}C$, followed by 1 day at $20\,^{\circ}C$, and 10 days at $4\,^{\circ}C$. Control twigs stored for 7 months at $-20\,^{\circ}C$ and subsequently stressed by $3\,^{\circ}C\ h^{-1}$ cooling to and warming from $-50\,^{\circ}C$ showed good survival (67%, $n = 43$).

Figure 2(a) shows the warming record after cooling at $120\,^{\circ}C\ h^{-1}$ to $-160\,^{\circ}C$. The $E'(-160)$ value is surprisingly high at 6.8 GPa. The ratios $E'(-60)/E'(-160)$ and $E'(-30)/E'(-60)$ are 0.70 and 0.81, respectively. The ratio of loss peaks $E''(u)/E''(l)$ is 2.2. Consistent with the modest E'' ratio, the absolute value of the loss modulus is also very high, as for the $42\,^{\circ}C\ h^{-1}$ cooled sample (Fig. 1(b)). Thus, the low temperature E'' peak is about 300 MPa, whereas the high temperature peak is about 400 MPa. The $\tan\delta$ peak maxima are -112 and $-27\,^{\circ}C$. Thus, the twig behaves in much the same way as the $-42\,^{\circ}C\ h^{-1}$ cooled sample, in that the upper $\tan\delta$ peak is at a lower temperature than that of the very slowly cooled twigs. The $E''(u)/E''(l)$ ratio is about the same as for the $42\,^{\circ}C\ h^{-1}$ cooled twig. There is more evidence that some devitrification is occurring between -60 and

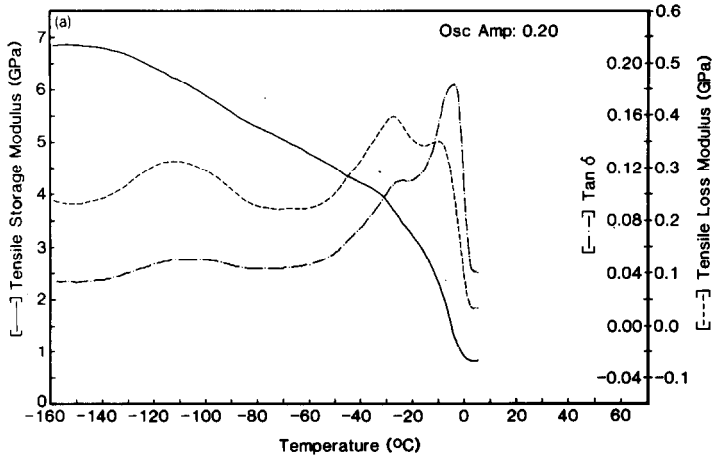
(a)
Osc Amp: 0.20
[——] Tensile Storage Modulus (GPa)
[– –] Tan δ
[– – –] Tensile Loss Modulus (GPa)
Temperature (°C)

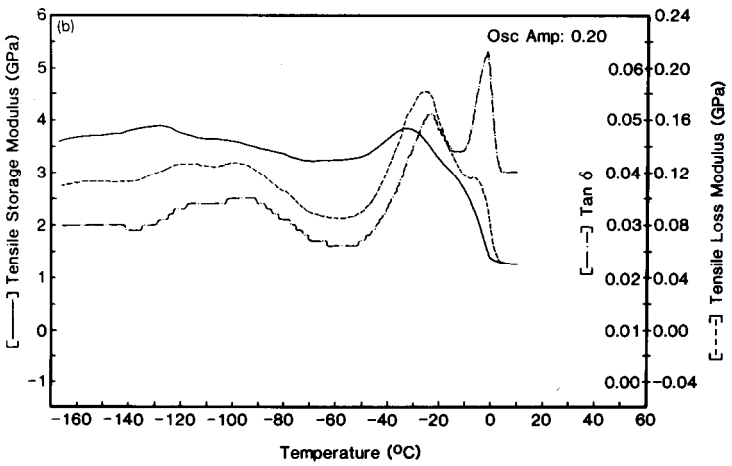
(b)
Osc Amp: 0.20
[——] Tensile Storage Modulus (GPa)
[– –] Tan δ
[– – –] Tensile Loss Modulus (GPa)
Temperature (°C)

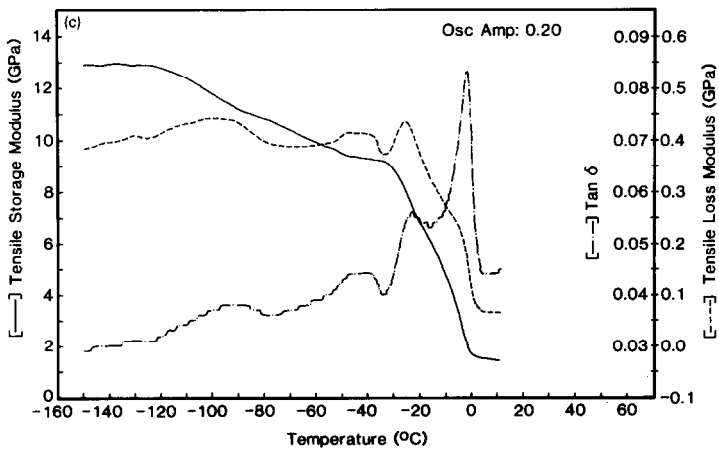
(c)
Osc Amp: 0.20
[——] Tensile Storage Modulus (GPa)
[– –] Tan δ
[– – –] Tensile Loss Modulus (GPa)
Temperature (°C)

$-30\,^{\circ}C$ than was the case after $42\,^{\circ}C\ h^{-1}$ cooling, because $E'(-30)/E'(-60)$ is 33% higher in this sample.

Figure 2(b) shows a twig from the same group as shown in Fig. 2(a). This twig was cooled at $600\,^{\circ}C\ h^{-1}$ to $-160\,^{\circ}C$. There are two low temperature $\tan\delta$ peaks at -117 and $-100\,^{\circ}C$. The high temperature $\tan\delta$ peak has a maximum at about $-24\,^{\circ}C$. The storage modulus curve shows a very low $E'(-160)$ value of 3.6 GPa, followed by a monotonic increase from -160 to $-130\,^{\circ}C$. We believe stiffening below $-130\,^{\circ}C$ may be due to crack healing in the intracellular aqueous glasses [5]. Above $-60\,^{\circ}C$ E' increases markedly, so the E' ratios are correspondingly high: $E'(-60)/E'(-160) = 0.89$, and $E'(-30)/E'(-60) = 1.20$.

The $E''(u)/E''(l)$ ratio is 4.3. The absolute value of the E'' peaks is less abnormal, the low temperature peak being 115 MPa and the high temperature peak 180 MPa.

Fig. 2(a). Warming record for a 40×3.25 mm fully hardy twig held for 7 months at $-20\,^{\circ}C$, thawed at a mean rate of $0.07\,^{\circ}C\ h^{-1}$, then refrozen in the DMA at $120\,^{\circ}C\ h^{-1}$ to $-150\,^{\circ}C$. $E'(-160)$ is moderate at 6.8 GPa. The EM evidence from a congeneric twig run simultaneously (Figs. 3(d) and (e)) indicates intracellular freezing in about half the cells. Nevertheless, there is little overt stiffening here since E' is monotonic decreasing throughout the record. However, while $E'(-60)/E'(-160)$ is a relatively low 0.70, $E'(-30)/E'(-60)$ is 0.81, indicating that some significant devitrification may have occurred above $-60\,^{\circ}C$. Also $E''(u)/E''(l)$ is 2.2, indicating reduced liquidity at low temperatures. The subzero lower temperature $\tan\delta$ peak is at $-112\,^{\circ}C$ and the upper one is at $-26\,^{\circ}C$, but neither appears abnormal in shape. Oscillation amplitude was 0.5 mm.

Fig. 2(b). A fully hardy twig, 40×6.8 mm, stored for 7 months at $-20\,^{\circ}C$, thawed at a mean rate of $0.07\,^{\circ}C\ h^{-1}$, then refrozen in the DMA at $600\,^{\circ}C\ h^{-1}$ to $-150\,^{\circ}C$. A twig for EM analysis which was run simultaneously showed massive cytoplasmic freezing and some intraorganellar freezing (Fig. 3(f)). This DMA record closely resembles the $120\,^{\circ}C\ h^{-1}$ cooled freshly collected samples. $E'(-160)$ is very low at 3.6 GPa. E' increases steadily up to $-130\,^{\circ}C$, implying crack healing in intracellular glasses. The ratio $E'(-60)/E'(-160)$ is high at 0.89, implying devitrification. The ratio $E'(-30)/E'(-60)$ is 1.20, reflecting significant devitrification in that temperature range. $E''(u)/E''(l)$ is 4.3, also indicating a reduction in liquefaction during warming below $-60\,^{\circ}C$, as compared to samples cooled more slowly.

Fig. 2(c). Warming record of a hardy twig stored at $-20\,^{\circ}C$ for 7 months, thawed at $0.07\,^{\circ}C\ h^{-1}$, then recooled at $600\,^{\circ}C\ h^{-1}$ to $-150\,^{\circ}C$, rewarmed rapidly to $-70\,^{\circ}C$, held for 1 h, and then recooled rapidly to $-150\,^{\circ}C$. The record resembles freshly collected material cooled to $-150\,^{\circ}C$ at $90\,^{\circ}C\ h^{-1}$, then warmed at $18\,^{\circ}C\ h^{-1}$ until $-70\,^{\circ}C$ (Fig. 1(d)). A distinct intermediate peak has appeared in both the loss curve and the $\tan\delta$ curve. $E'(-160)$ is 13 GPa, consistent with complete devitrification in low T_g subdomains. Also, $E'(-60)/E'(-160)$ is quite low at 0.76. $E'(-30)/E'(-60)$ is high at 0.92, indicating continued devitrification above $-70\,^{\circ}C$. Neither the very small size of the loss peaks, nor the generally high level of loss throughout the range can be explained by our models. Oscillation amplitude was 0.20 mm.

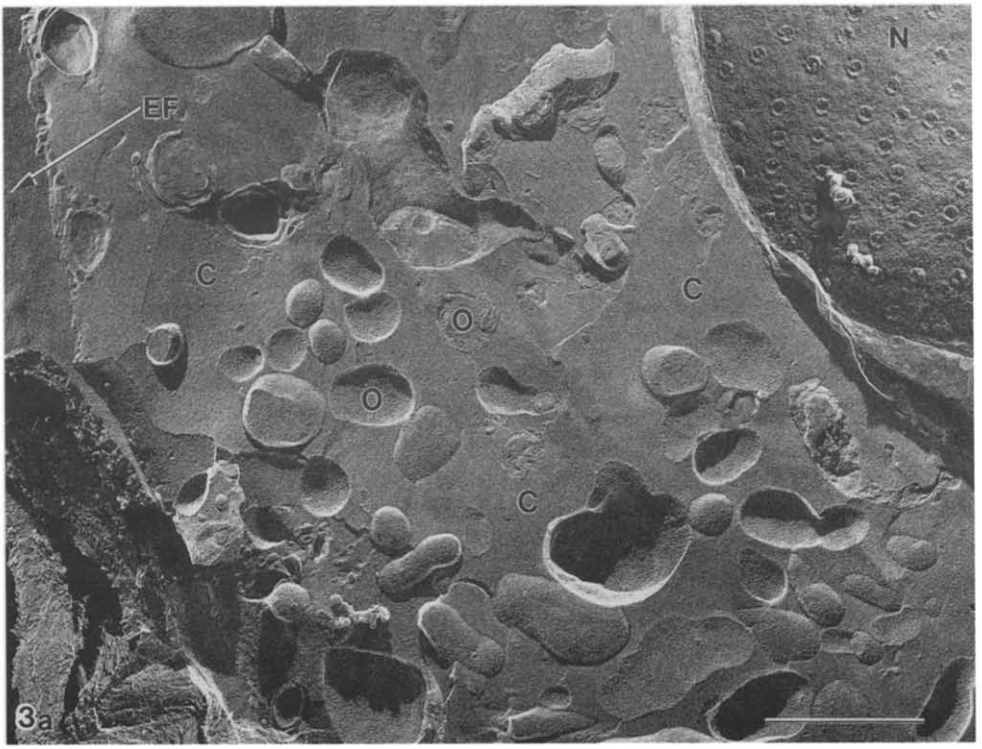
N
EF
C
C
O
O
C
3a


CW
O
O
O
C
C
C
3b

Figure 2(c) shows what happens when a sample from the same group of twigs as shown in Figs. 2(a) and (b) is cooled at 600 °C h^{-1} to −150 °C, warmed at the same rate to −70 °C, held for 1 h, and then recooled at 600 °C h^{-1} to −150 °C with no working. The results most clearly resemble Fig. 1(d), the fresh twig cooled while being worked at 90 °C h^{-1} to −150 °C, and then rewarmed to −70 °C while working at 18 °C h^{-1}. There

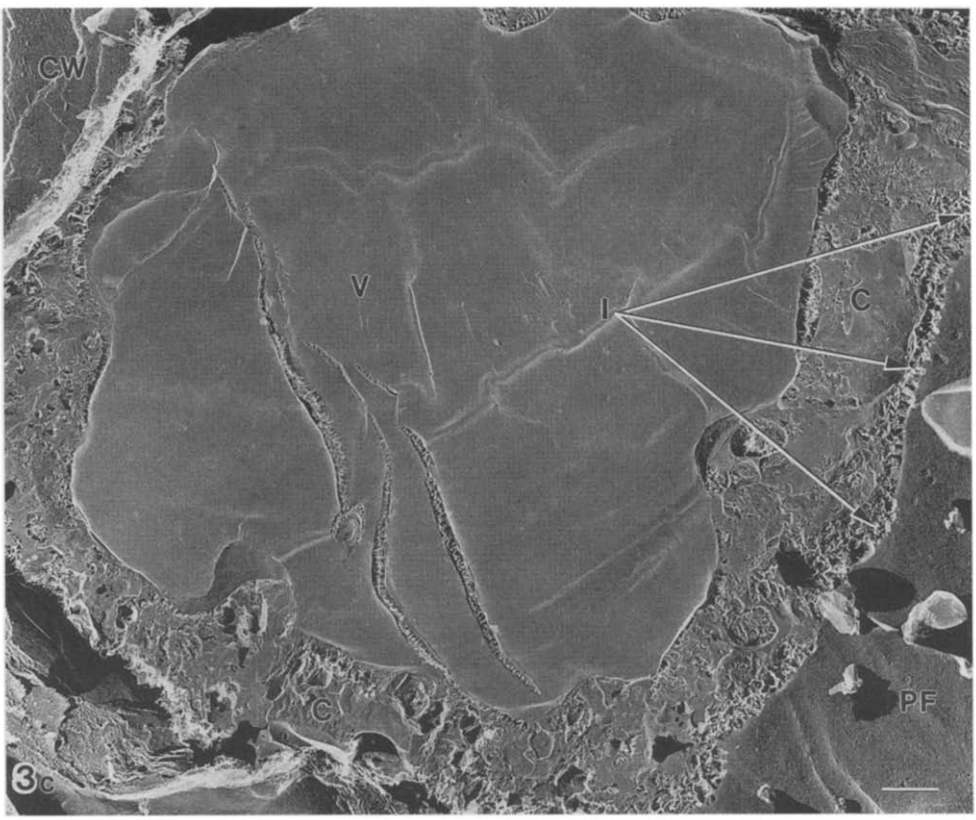

Fig. 3(a). Cross-section of a cell from fully hardy freshly collected *Populus* cooled to −70 °C at 3 °C h^{-1}. The cytoplasm (C) is smooth, showing no indication of intracellular ice. Membranes appear undistorted and MAPs evenly distributed in organelles (O), the nuclear membrane (N), and the outer leaflet of the plasma membrane (Ef). Bar = 1 μm.

Fig. 3(b). Fully hardy freshly collected *Populus* cooled at 42 °C h^{-1} to 50 °C, then stored at −80 °C. Upper left corner is cell wall (CW). The rest is cytoplasm (C) and packed organelles (O). There is no evidence of any intracellular ice. Bar = 1 μm.

Fig. 3(c). A fully hardy freshly collected twig cooled at 55 °C h^{-1} to −50 °C, then stored at −80 °C. The cross-fractured cell shown here displays massive intracellular freezing (holes) (I). Ice is concentrated under the inner plasma membrane leaflet (PF), and there is cytoplasm (C) relatively free of ice. The vacuole (V) is the digestive system of the cell. It appears free of ice. Outer regions of the micrograph include the cell wall (CW). Bar = 1 μm.

are three clearly defined tan δ peaks below 0 °C, at −94, −46 and −25 °C. The $E''(u)/E''(l)$ ratio is 0.5. This ratio is very different from that of previous samples. Also, the loss modulus is unusually high, at about 400 MPa throughout the temperature range, and the peak heights above background are much smaller than in the other samples. $E'(-160)$ is 13 GPa, the highest storage modulus we have seen. The ratios $E'(-60)/E'(-160)$ and $E'(-30)/E'(-60)$ are 0.76 and 0.90 respectively implying that low temperature devitrification has proceeded nearly to completion, but devitrification above −50 °C is still significant.

Fig. 3(d). A fully hardy twig stored for 7 months at −20 °C, warmed at 0.07 °C h^{-1}, held for 1 day at 20 °C, and then recooled at 120 °C h^{-1} to −150 °C. About half of the cells showed the massive cytoplasmic freezing (I) shown here. Despite the extensive freezing, the cross-fractured vacuole (V) on the left shows no freezing, and some areas of the cytoplasm (C) are also relatively free of ice. The large region to the right is the inner leaflet of the plasma membrane (Pf), identified by the presence of plasmadesmata (Pd). Bar = 1 μm.

Electron microscopy

Freeze-etch electron micrographs allow one to ascertain the subcellular localization of ice, if any intracellular ice is present, after exposing twigs to various rates of cooling.

Figure 3(a) shows the interior of a cell from a fully cold-resistant twig cooled at $3\,^{\circ}C\ h^{-1}$ to $-70\,^{\circ}C$. From the cell wall at the lower left through the cytoplasm to the nucleus on the upper right there is no sign of ice formation. Ice formation would be indicated by the presence of holes where ice had sublimed away as a result of etching prior to replica formation. This twig was saved after cracking, thawed, and held in growth medium. It calloused within three weeks.

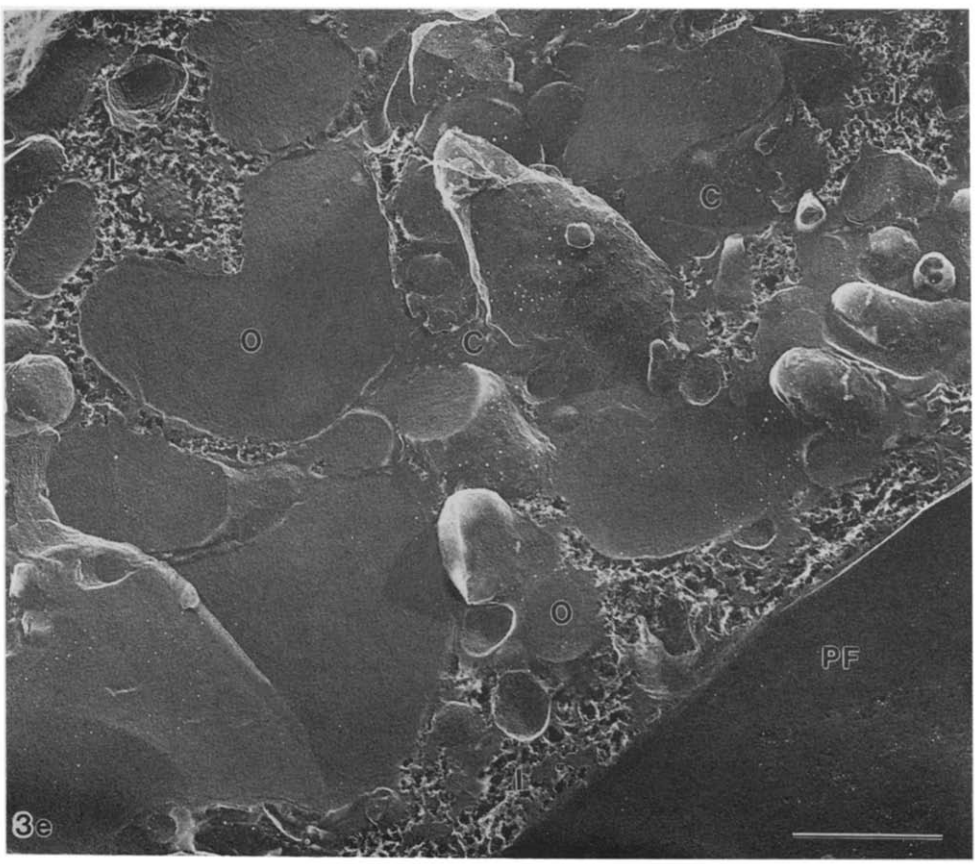

Fig. 3(e). The same $120\,^{\circ}C\ h^{-1}$ cooled twig as shown in Fig. 3(d). Much of the cytoplasm is massively frozen (I), but cross-fractured organelles (O) show no ice (I). Some areas of cytoplasm also remain unfrozen (C). In the lower right corner, the inner leaflet of the plasma membrane (PF) shows evidence of underlying ice because of the presence of holes. Bar = 1 μm.

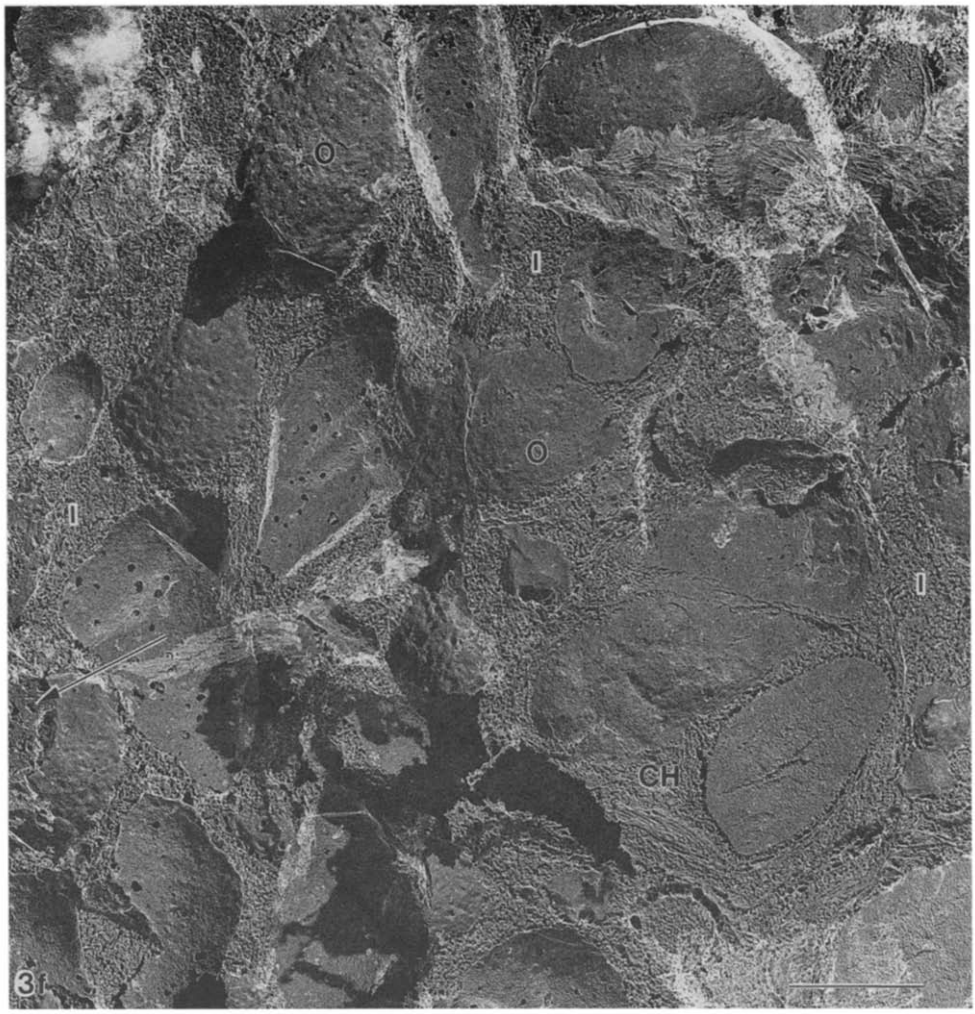

Fig. 3(f). A fully hardy twig stored at $-20\,^{\circ}C$ for 7 months, thawed at $0.07\,^{\circ}C\ h^{-1}$, held for 1 day at $20\,^{\circ}C$, and then recooled to $-150\,^{\circ}C$ at $600\,^{\circ}C\ h^{-1}$. This is a cytoplasmic field with cross-fractured organelles (O). The cytoplasm is more massively frozen (I) than in the $120\,^{\circ}C\ h^{-1}$ material and organelles show some intracompartmental freezing, as evidenced by holes in the organelles' Ef face and holes in the inner content of cross-fractured organelles such as chloroplasts (arrow and CH). Bar = 1 μm.

Figure 3(b) shows a part of the cytoplasmic compartment of a twig cooled at $42\,^{\circ}C\ h^{-1}$ to $-50\,^{\circ}C$, and then stored in dry ice. The survival of these twigs was 76% ($n = 17$). There is no evidence of intracellular ice formation in these samples.

Figure 3(c) shows a cross-fractured cell from a fully hardy twig cooled at $55\,^{\circ}C\ h^{-1}$ to $-50\,^{\circ}C$, and then stored in dry ice. The survival of this group of twigs was 50% ($n = 14$). Approximately half of the cells examined in this twig displayed extensive intracellular freezing in the cytoplasmic compart-

ment. Compartments such as vacuoles and chloroplasts displayed almost no freezing. Ice crystal formation is heaviest just below the surface of the plasma membrane, implying sudden freezing of cytoplasmic contents owing to the invasion of ice from the extracellular space.

At the time these studies were conducted, 55 °C h^{-1} to −50 °C was the maximum controlled rate we could achieve with our cooling baths. The DMA records for freshly collected material were made in the expectation that simultaneous 90 and 120 °C h^{-1} cooling studies would be completed in the DMA using the LNCA; concurrent samples would then be examined by EM. In fact, a successful 120 °C h^{-1} EM run was not completed until the twigs had been stored for 7 months at −20 °C. By this time, as is clear from Fig. 2(a), the DMA record for a 120 °C h^{-1} cooled twig showed less evidence of devitrification than that for freshly collected twigs cooled at the same rate (Figs. 1(c) and (d)).

The EM data show that intracellular ice formation in freshly collected and −20 °C stored twigs cooled at 120 °C h^{-1} is strikingly similar. Figure 3(d) shows a partially frozen cytoplasmic region bordered by an unfrozen vacuolar region in −20 °C stored material thawed at 0.07 °C h^{-1}, held for 1 day at 20 °C, and then recooled at 120 °C h^{-1}. Figure 3(e) shows another cell in the same twig. Here also there is extensive cytoplasmic freezing, but organellar contents are unfrozen.

When we cooled twigs which had been thawed at 0.07 °C h^{-1} after 7 months at −20 °C at still higher rates (600 °C h^{-1}), the DMA records once again correlated well with those for freshly collected hardy material cooled at 90 and 120 °C h^{-1}. Compare Figs. 1(c) and (d) to Fig. 2(b). The EM record for 600 °C h^{-1} cooled −20 °C stored material (Fig. 3(f)) showed a significant increase in cytoplasmic ice and intraorganellar ice. Thus, increasing the cooling rate increases intracellular ice content during freezing, as shown by EM data, and ice formation during thawing, as shown by DMA data.

Differential scanning calorimetry

Populus samples are far too chemically complex for it to be possible to construct models explaining their behavior in the DMA directly from the data. Perhaps the simplest model system to use for comparison would be water; one of the major storage sugars, such as raffinose; the prevailing intracellular electrolyte, KCl; and one highly soluble protein. We used bovine serum albumin (BSA) because it is soluble at very high concentration and not denatured by freezing. We studied glass transitions in these quaternary solutions, and in simpler solutions, with the concentration of each of the components closely approximating the concentration of that class of component in vivo. We used DSC to perform the studies because we have as yet been unable to develop a container which is sufficiently

mechanically inert to allow proper monitoring of frozen solutions in the DMA.

Figure 4(a) shows the results of heating a quaternary solution of H_2O : raffinose : BSA : KCl of composition 8 : 2 : 1 : 0.12 in the DSC after 6000 °C h^{-1} cooling (dashed line). The solid curve shows warming of the same sample after 6000 °C h^{-1} cooling to −160 °C, followed by annealing for 5 min at −35 °C, and then rapid recooling. The unannealed solution shows no detectable thermal transition until −60 °C is reached, at which point an endotherm commences. At about −42 °C the endotherm peaks and

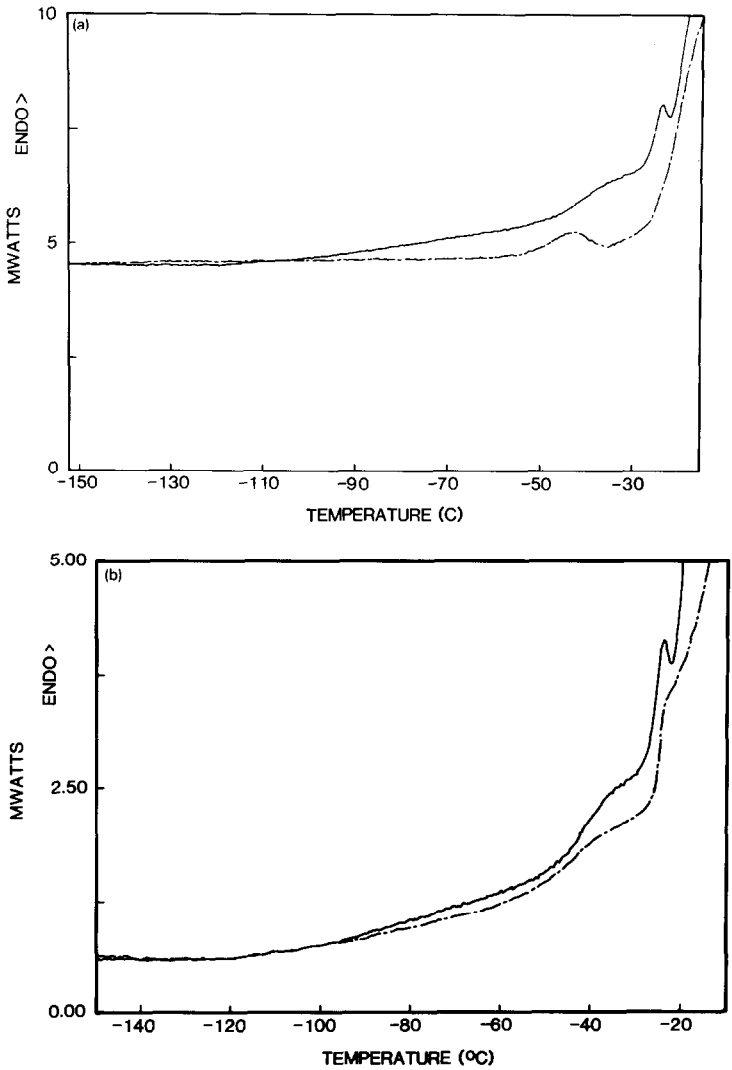

Fig. 4.

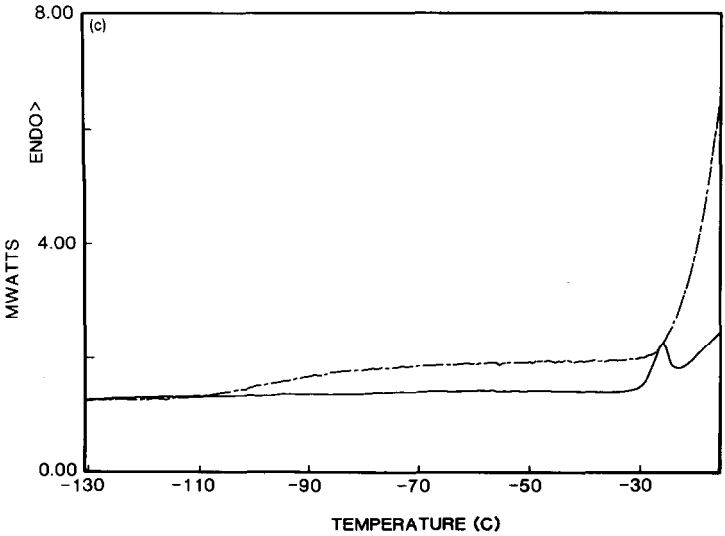

Fig. 4(a). The solid curve is the 300 °C h^{-1} DSC warming curve of a quaternary solution of H_2O:raffinose:BSA:KCl in ratio 8.19:2:1:0.12 by weight cooled at 6000 °C h^{-1} to −160 °C, rewarmed at the same rate to −35 °C, held for 5 min, and recooled at the same rate to −160 °C. The dashed curve is the same sample warmed at 300 °C h^{-1} after 6000 °C h^{-1} cooling only. Note that detectable heat capacity increases begin at −60 °C in the quickly cooled sample, but at −115 °C in the −35 °C annealed sample. The annealed sample shows a slow heat capacity increase from −115 to −45 °C which is probably the softening of protein-enriched subdomains. Another transition, beginning at −46 °C, is a glass transition in a subdomain which is probably close to the initial unfrozen solution in terms of sugar:protein ratio. A sugar-enriched transition begins at −28 °C, and a final endotherm begins at −22 °C. By contrast, the quickly cooled sample shows an exotherm following the initial endotherm, indicating devitrification. There is only a hint of formation of a sugar-enriched domain in the form of a faint shoulder at −26 °C.

Fig. 4(b). The same quaternary solution as shown in Fig. 4(a). The solid curve represents 3000 °C h^{-1} warming after cooling at 6000 °C h^{-1}, followed by annealing at −35 °C. The dashed curve is for warming at 120 °C h^{-1} after cooling at 120 °C h^{-1}. Note that, as for the 6000 °C h^{-1} cooled material annealed at −35 °C, the slowly cooled sample shows several endothermic transitions during warming. However, the 120 °C h^{-1} cooled material seems to develop a more dilute intermediate composition (higher water content), as evidenced by the onset of a larger endotherm at a lower temperature. Also, the highest temperature glass transition lacks an overshoot characteristic of annealed material. These results show that phase separation has time to occur in a complex solution suddenly frozen at high subzero temperatures and subsequently cooled at 120 °C h^{-1}.

Fig. 4(c). The solid curve is for a ternary solution of raffinose (21.5%), stachyose (21.5%) and water, cooled at 6000 °C h^{-1}, annealed at −35 °C, recooled, and then warmed at 600 °C h^{-1}. The dashed curve is for a ternary solution of BSA (20%), 0.2 M KCl and water, cooled at 6000 °C h^{-1}, annealed at −32 °C, recooled, and then warmed at 300 °C h^{-1}. This record illustrates why we think that the very low temperature transitions in both model solutions and wood are protein-dominated, while the high temperature transitions are either mixtures or sugar-dominated. The glass transition in the protein–salt solution is near −110 °C, while that of the sugar–water solution is above −30 °C.

exothermic behavior, devitrification, begins. The exotherm reaches a minimum at about −35 °C. A sharp increase in endothermic behavior begins at −28 °C, with a slight reduction in slope at −23 °C. By contrast, the same sample cooled quickly to −160 °C, warmed and then annealed at −35 °C before recooling shows very different thermal behavior. An endothermic ramp begins at −120 °C and proceeds almost linearly to −46 °C, at which point an increase in endothermic activity begins. A very steep endotherm commences at −28 °C, peaking at −24 °C. The final endotherm commences at −22 °C. There is no detectable exothermic behavior remaining. These records imply that if freezing is very rapid and incomplete, a relatively well mixed glassy solution unstable to continued ice formation remains between ice crystals. On warming, this solution shows one glass transition followed by an exotherm. If, on the other hand, the freezing is allowed to go to completion in the temperature range of devitrification, then liquid–liquid phase separation occurs and multiple glass transitions are seen in the solution.

Figure 4(b) is an exploration of the effects of freezing rate on liquid phase separations in the quaternary solution. The solid curve is the same as the solid curve of Fig. 4(a), i.e. the warming curve of a solution cooled at 6000 °C h^{-1} to −160 °C, rewarmed to −35 °C for 5 min, and then rapidly recooled to −160 °C. The dashed curve shows the warming curve of the same quaternary solution cooled at 120 °C h^{-1} to −160 °C followed by warming at 120 °C h^{-1}. The most important aspect of the comparison is the generally analogous thermal transition structure of the two systems. Both display a broad low temperature endotherm—almost a ramp—between −120 and −60 °C. Above −60 °C a second endotherm appears, with a third appearing at about −28 °C. In the slowly cooled sample, the middle endotherm commences about 10 °C lower, and the highest endotherm lacks an overshoot. These results are consistent with phase separation having gone nearly to completion in both samples, but having proceeded further in the −35 °C annealed sample.

Figure 4(c) shows why we think the three endotherms in the phase-separated quaternary solution represent three phases with increasing sugar content at progressively higher temperature transitions. The dashed curve represents a −35 °C annealed ternary solution of 20% BSA and 0.2 M KCl. The glass transition is a simple broad endotherm from −120 to −85 °C. What we assume to be equilibrium melting of ice becomes detectable at about −25 °C. In comparison, the solid curve is of a 20% raffinose (binary) solution annealed at −35 °C after quick cooling to −160 °C. The glass transition begins at about −35 °C and peaks, with an overshoot, at about −25 °C. Thus, the curve for the pure sugar solution looks very much like the endotherm which peaks at −24 °C in the fully phase-separated quaternary solution, whereas the curve for the protein–salt solution looks much the

same as the lowest temperature endotherm of the phase-separated quaternary solution.

DISCUSSION

The DSC investigations of model solutions strongly suggest that in the frozen state these solutions form multiple domains with differing glass transitions. It is not hard to envisage a mechanism for this. Ice crystals form suddenly in the under-cooled solutions. As the crystals grow rapidly towards one another at high cooling rates the large differences in mobility between salts, sugar and proteins produce large concentration gradients extending from the crystal faces into the solution. This in turn is likely to lead to liquid–liquid phase separation during devitrification, such as spinodal decomposition [6–11]. The positions of the glass transitions in the model quaternary solutions imply that domains form with a compositional range from nearly pure aqueous protein and salt to nearly pure aqueous sugar and salt.

The biological material is of course much more complicated than the model solutions. Considering this, it is remarkable how closely the DMA and DSC data coincide. The DMA data for hardy twigs cooled at non-lethal (slow) rates display a broad low temperature transition in the same range as the transition in the aqueous protein solutions. Even the $\tan\delta$ peak falls at about the midpoint of the aqueous BSA–KCl glass transition as measured by DSC. The shoulders in the DMA record at -45 and $-23°C$ are consistent with the sugar-associated glass transitions in the quaternary model solution.

When analysing the extent of congruence between the DMA records of wood frozen at a lethal rate and the DSC records of model solutions cooled at a high rate, it is important to consider first the microanatomy of the wood. Figure 5 shows the structure of the basic *Populus* cell in cross-section [12], as well as its response to osmotic stress in both the hardy (winter) and non-hardy (summer) states. The cell wall is outside the living cell proper, in much the same way as a turtle's shell is outside the turtle. Nevertheless, light microscope observations (not shown) and EM observations (Figs. 3(a)–(f)) show that in wood cooled at non-lethal rates the cell membranes adhere to the cell wall. This causes the cell walls to collapse as water leaves the cells to freeze exclusively in the extracellular space. Since the cell wall is the structurally strong part of wood as long as the cell interiors are liquid, the cell membrane is doing considerable work on the wall to collapse it. If the wood is cooled at ever increasing rates this may lead to a critical power function beyond which tearing of the cell membrane can be expected. At the same time, the faster the cooling rate, the less time water has to leave the cell, both because of diffusional limitations and because the cell wall resists

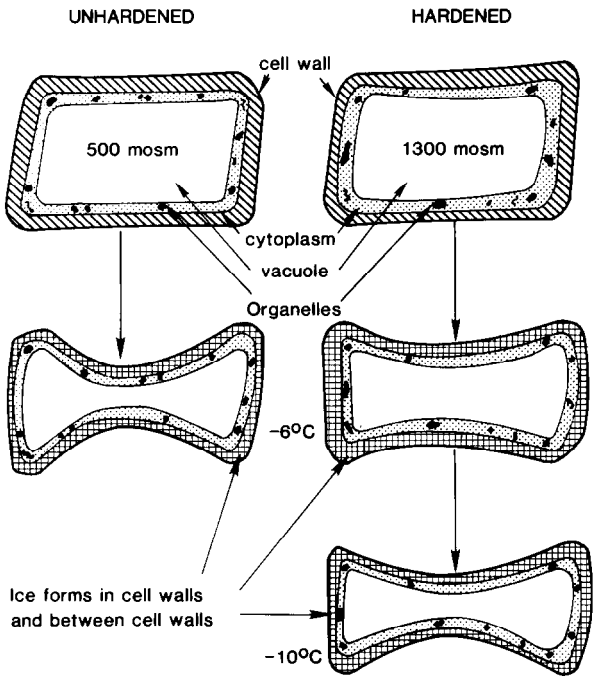

Fig. 5. An illustration of the basic structure of living *Populus* cells. During the growing season the outer jacket is extruded from the cell proper. This is the cell wall and the structural part of wood. Immediately within this shell and adpressed to it is the plasma membrane, similar to that found in all eucaryotic cells. Just within the plasma membrane is the cytoplasm, the living metabolic fluid of the cell proper. This is filled with special functional entities, called organelles, encased in their own membranes. These include chloroplasts, mitochondria, golgi bodies, peroxisomes, nuclei and vacuoles. The vacuoles may be coalesced into one enormous central organelle which can occupy 90% of the cell's volume, as shown here. The intracellular freezing point depression is 1300 mosm in the winter, and $\leqslant 500$ mosm in the summer. Thus, the winter cell loses a much smaller fraction of its initial water to extracellular ice at a given subfreezing temperature. The figure depicts this as reduced cellular collapse. Note also that in both hardy and non-hardy cells the plasma membrane sticks to the cell wall and collapses in with it. Thus, the cell does work on its cell walls as freezing progresses. (Reproduced with the permission of Academic Press from ref. 12.)

collapse. This leads to increasing supercooling of the aqueous intracellular medium. On this basis we hypothesize that tearing of the plasma membrane at a temperature significantly below 0 °C will lead to rapid freezing of the cytoplasmic contents. According to this view, the ice crystals would be close to the inner surface of the plasma membrane. Since the mechanical stress is not directly applied to organellar membranes, these would be expected to show resistance to intracompartmental freezing at rates that are rapid enough to freeze the cytoplasm, but still fairly slow. The EM results support these assumptions. More extreme rates of cooling would lead to increased supercooling, especially in compartments embedded deeply in the bulk of the cells. Sudden freezing of the cytoplasm under such circumstances would

lead to large water activity gradients between intraorganellar compartments, and a suddenly concentrated cytoplasm. There is evidence that in cellular suspensions lacking cell walls (protoplasts), large osmotic gradients across the plasma membrane (sudden extracellular freezing) produce fibrillation and membrane failure owing to hydraulic flow stresses through the membrane [13]. Extreme membrane stress in such systems appears to allow ice to penetrate the membrane barrier and grow intracellularly. In a similar fashion, we postulate, intraorganellar spaces will freeze during rapid cooling following a sudden cytoplasmic freeze. The EM results for $55\,^{\circ}C\ h^{-1}$ and $120\,^{\circ}C\ h^{-1}$ cooling (Figs. 3(c) and 3(d) and (e) respectively) show little or no intraorganellar freezing. In contrast, and in support of this hypothesis, Fig. 3(f) shows intraorganellar freezing in $600\,^{\circ}C\ h^{-1}$ cooled material.

The DSC results are consistent with a model which suggests that non-lethal cooling produces concentration gradients through the intracellular solutions leading to liquid–liquid phase separation. If cooling is too quick, this process is kinetically inhibited by sudden invasion of supercooled cells by ice. This leads to solutions showing phase transitions more characteristic of a quickly frozen and relatively well mixed sugar–protein–salt model solution. The expected change in the DMA record is a reduction in the very low temperature loss peaks and a region of devitrification and high loss between -70 and $-20\,^{\circ}C$. This is what we seen in Figs. 1(c) and (d) and 2(a)–(c), as illustrated by E' and the $E''(u)/E''(l)$ ratios.

Another set of data in support of interrupted liquid phase separations during fast cooling of *Populus* is the comparison of Fig. 1(d) with Fig. 2(c). In both of these samples, fast cooling was followed by very slow warming to $-70\,^{\circ}C$, or annealing for 1 h at $-70\,^{\circ}C$ followed by recooling. These records both show significant $\tan\delta$ and loss peaks at $-50\,^{\circ}C$. We interpret this to mean that phase separation has been partial at very low temperatures where only high protein and low sugar content phases could separate. Phases of intermediate composition are probably represented by the loss peaks near $-80\,^{\circ}C$ in the fast cooled samples (Figs. 1(c) and 2(b)). These phases would dehydrate during slow warming or annealing to $-70\,^{\circ}C$ and their relative sugar content would probably increase. They would thus be expected to yield a new peak between -70 and $-30\,^{\circ}C$, which is what the data show.

It is at first somewhat puzzling that higher cooling rates are required to achieve the same general DMA result in wood stored for 7 months at $-20\,^{\circ}C$ as opposed to freshly collected wood. However, this is consistent with the idea that continuous tension in the cell walls for so long a period at $-20\,^{\circ}C$ has led to creep, i.e. plastic deformation. The walls would therefore display a lower elastic constant when restressed by cellular collapse during a second freeze. This increase in cell wall compliance would reduce the stress rate maximum at a given cooling rate, leading to a reduced number of cells actually freezing intracellularly and a reduced amount of ice formation and subsequent devitrification in those that did freeze intracellularly. This is

consistent with a DMA record more like that for slowly cooled material, as illustrated by Fig. 2(a). It is also consistent with our observation that the $-20\,^{\circ}C$ stored wood cooled at $120\,^{\circ}C\ h^{-1}$ showed freezing in only half of the cells examined by EM. The $600\,^{\circ}C\ h^{-1}$ cooled, $-20\,^{\circ}C$ stored material would be expected to develop a high stress rate despite its increased compliance because of the greatly increased cooling rate. The challenge is to explain why this leads to intraorganellar freezing while $120\,^{\circ}C\ h^{-1}$ cooling of freshly collected or $-20\,^{\circ}C$ stored twigs does not. We believe the answer lies in the previously stated idea that the organelles are not doing work on the cell wall. Their membranes are therefore unlikely to tear at cooling rates as low as $120\,^{\circ}C\ h^{-1}$. At higher rates the membranes, like the cytoplasmic compartment, would be increasingly supercooled. Upon sudden freezing of the cytoplasm a large osmotic gradient would develop very rapidly from the intraorganellar spaces to the cytoplasm. Then the hydraulic stresses themselves could lead to intolerable membrane stress and subsequent invasion by ice.

The E' analysis supports and extends our hypothesis. The data indicate that 65% of the stiffness of a slowly cooled, hardy twig (Fig. 1(a)) is the result of cooling from -30 to $-150\,^{\circ}C$. Analysis of the ice melting peaks of slowly cooled *Populus* [4] indicates that during slow cooling to $-20\,^{\circ}C$, 90% of the total water content turns to ice. Thus, the stiffness below $-30\,^{\circ}C$ is not due to additional ice formation. It must be primarily due to increases in intracellular viscosity consistent with intracellular glass formation. The E' ratios indicate that about 40% of the stiffening occurs between -30 and $-60\,^{\circ}C$ and 60% between -60 and $-150\,^{\circ}C$. This does not necessarily mean that more liquid solidifies below $-60\,^{\circ}C$ than above $-60\,^{\circ}C$, because the microdomains that go through a glass transition at about $-25\,^{\circ}C$ will continue to stiffen well below the solid–liquid phase transition, contributing to the rise in the bulk modulus.

The E' ratios in the wood cooled at a lethal rate are high throughout the range -150 to $-30\,^{\circ}C$. If significant devitrification occurred in these samples, the E' curves indicate that most of it occurred above $-60\,^{\circ}C$. However, the high $E'(-60)/E'(-160)$ ratios in quickly cooled wood might indicate additional devitrification only in protein-dominated subdomains of high water content. Alternatively, it could indicate that, because of a failure to phase separate, few domains have a high enough relative protein content to achieve very low temperature glass transitions, so that E' stays high. We favor the latter hypothesis. The absolute E' values at very low temperatures are also consistent with our hypothesis. They are consistently lower for quickly cooled samples. In general, in hardy samples the faster the cooling, the lower the modulus. If less water freezes to ice, this would of course reduce the very stiff crystalline water phase. In addition, it would yield intracellular aqueous glass-forming solutions with higher water contents. Since water is a plasticizer in this circumstance, this would lead to a

reduction in stiffness in the resultant glasses. If most of the stiffness in these samples were determined by the amount of unfreezable water bound to cell walls, one would expect a much higher residual stiffness after thawing. Furthermore, reducing the amount of water going from cellular interiors to cell walls by fast cooling would be expected to increase cell wall stiffness—yet quickly cooled samples show significantly less stiffness below $-30\,^{\circ}C$.

We do not have a good explanation of the large variability in E' after thawing, although 1.0–1.5 GPa seems to be the most reliable value. The very high loss levels of the $120\,^{\circ}C\ h^{-1}$ cooled, $-20\,^{\circ}C$ stored sample (Fig. 2(a)), the $600\,^{\circ}C\ h^{-1}$ cooled, $-70\,^{\circ}C$ annealed sample (Fig. 2(c)) and the $42\,^{\circ}C\ h^{-1}$ cooled, freshly collected sample are also beyond the explanatory capability of our crude model.

CONCLUSIONS

Our DSC studies indicate that model protein–KCl–sugar solutions display one glass transition subsequent to fast cooling ($6000\,^{\circ}C\ h^{-1}$), but several glass transitions subsequent to slow cooling ($120\,^{\circ}C\ h^{-1}$) or fast cooling followed by annealing at $-35\,^{\circ}C$ and then recooling. We also see several glass transitions in DMA analysis of slowly ($3\,^{\circ}C\ h^{-1}$) cooled *Populus* wood. The DMA record for the wood changes drastically when it is cooled quickly enough to freeze the cytoplasm quickly, as shown by correlating EM with DMA results. The low temperature loss transitions are reduced in magnitude and significant evidence for devitrification (stiffening) occurs at temperatures above $-60\,^{\circ}C$ in the quickly cooled samples. Thus, the quickly cooled wood appears more like the quickly cooled model solutions.

These results lead us to postulate that during slow cooling to very low temperatures, *Populus* cytoplasm displays liquid–liquid phase separations leading to sugar–rich, protein–poor and sugar–poor, protein–rich microdomains. This means that parts of the cytoplasm are glassified during slow cooling to $-30\,^{\circ}C$, while other parts remain fluid to temperatures below $-100\,^{\circ}C$. This may mean that very long term storage in these tissues is limited to temperatures below $-100\,^{\circ}C$. It may also mean that the extreme cryoprotection afforded by the intracellular milieu in the winter dormant state is dependent on an orchestrated phase separation of sugars, salts and proteins.

ACKNOWLEDGEMENTS

We would like to thank Harold T. Meryman for a critique of the paper. Dr Robert J. Williams generously allowed us to present much of this work at

the 17th Annual NATAS meeting in Orlando, Florida. Christopher Pooley kindly prepared our micrographs for publication. The owners of Tri-State Stone Quarry in Potomac, Maryland have graciously allowed us unrestricted access to their large *Populus* grove.

This work was supported in part by National Institute of Health grants BSRG 2SO7, RROS737 and GM 17959.

REFERENCES

1 A. Bonicel, G. Haddad and J. Gagnaire, Plant Physiol. Biochem., 25 (1987) 451.
2 A.S. Fege and G.N. Brown, Forest Sci., 30 (1984) 999.
3 A.G. Hirsh, R.J. Williams and H.T. Meryman, Plant Physiol., 79 (1985) 41.
4 A.G. Hirsh, Cryobiology, 24 (1987) 24.
5 R.J. Williams and D.L. Carnahan, Thermochim. Acta, 155 (1988) 103.
6 J.W. Cahn and J. Hilliard, J. Chem. Phys., 28(2) (1958) 258.
7 J.W. Cahn, J. Amer. Ceram. Soc., 52(3) (1969) 118.
8 D. de Fontaine, in N.B. Hannay (Ed.), Treatise on Solid State Chemistry, Vol. 5: Changes of State, Plenum Press, New York, Chap. 3, pp. 161–165, 1976.
9 J.E. Morral and J.W. Cahn, Acta Metall., 19 (1971) 1037.
10 J.A. Thomson, P. Schurtenberger, G.M. Thurston and G.B. Benedek, Proc. Nat. Acad. Sci. U.S.A., 84 (1987) 7079.
11 R. Vassoille, G. Vigier, A. El Hacadi, G. Thollet and J. Perez, J. Phys. (Paris), Colloq., 48: C1 (1987) 471.
12 J. Levitt, Responses of Plants to Environmental Stresses, Vol. 1: Chilling, Freezing and High Temperature Stresses, Academic Press, Orlando, 1980, p. 243.
13 M.F. Dowgert and P.L. Steponkus, Plant Physiol., 72 (1983) 978.